© Universiti Tun Hussein Onn Malaysia Publisher's Office

IJIE

Journal homepage: http://penerbit.uthm.edu.my/ojs/index.php/ijie

ISSN : 2229-838X e-ISSN : 2600-7916

The International Journal of Integrated Engineering

Improvement of the Results of Finite Element Method in Plate Analysis Using Mesh Sizing Modifying Function

Mohammad Hadi Bagherinejad[1*], Reza Kamgar[2]

[1]Department of Civil Engineering,
Shahid Rajaee Teacher Training University, Tehran, IRAN

[2]Department of Civil Engineering,
Shahrekord University, Shahrekord, IRAN

*Corresponding Author

DOI: https://doi.org/10.30880/ijie.2020.12.08.004
Received 4 January 2020; Accepted 31 March 2020; Available online 30 August 2020

Abstract: In the finite element methods (FEM), the mesh dimension, and the number of elements can impact on the responses of structures. In this paper, a procedure is proposed to modify the stiffness matric of the plate element based on the mesh geometry and mesh size for reducing the central deflection error. The procedure is based on the recent plate formulation called TTK9S6. For this purpose, the modifying coefficients are defined for the bending and shear stiffness matrices. The sensitivity of coefficients is investigated considering the changes in the thickness of the plate element, the mesh dimension, and also the type of supports. The analysis results prove that the values of the bending coefficient are more effective in comparison to the shear coefficient. Finally, a function is proposed to determine the bending and shear matric coefficients based on the values of the exact displacements. Various numerical studies indicate that the modifying function has significantly improved the performance of the plate element, especially for the plates with irregular and large mesh dimensions.

Keywords: Finite element model, plate, mesh geometry, modifying function

1. Introduction

In the finite element method, mesh dimensions and topology have significant effects on the results of the analysis. In continuum structures such as plates and shells, the results converge to the exact values when the meshing of structures is optimally selected small enough. A meshing is desirable if the meshes dimensions are small enough, and the created elements have equal dimensions. On the other hand, the analysis will be time-consuming when the mesh size is small. Also, in a meshing procedure, creating the elements with the same size is not always possible. Therefore, providing a method to modify the stiffness matrix by considering the size and number of elements could be useful.

The effects of mesh size have been studied in many fields, such as linear FEM, nonlinear FEM, and fracture mechanics. Clovgh and Tocher [1] studied the rectangular and triangle plate elements and the mesh size based on the Kirchhoff plate bending theory. Choi and Kwak [2] investigated the effects of mesh size on the nonlinear behavior of reinforced concrete structures. Kanapady et al. [3] proposed an initial approximate value for mesh density using the data mining techniques that there did not require any trial and error to start finite element computations. A relation between the critical strain to failure and the size of the "unit cell" was presented by Li et al. [4]. Nam *et al.* [5] presented mesh sensitivity on the structure subjected to the blast wave. Troyani et al. [6] investigated the effect of triangular finite element mesh orientation on the responses of solid and fluid mechanics. The effect of element size in numerical simulation of the incremental sheet-forming process was studied by Suresh and Regalla [7]. Antunes et al. [8] optimized the finite element mesh that was used to predict the plasticity-induced crack closure. Therefore, based on the literature mentioned earlier, it can be observed that several types of researches have been proposed on mesh size for analysis of structures. Recently, Perumal [9] introduced a new technique for Delaunay triangular mesh generation and element optimization. This method was implemented through the generation of sample points using mapping for Delaunay triangulation and mesh

**Corresponding author: mh.bagherinejad@sru.ac.ir/mh.bagherinejad@gmail.com*

optimization. Based on the literature mentioned above, it should be noted that the mesh size has an important effect on the responses of both static and dynamic problems [10-13].

The plate and shell structures are widely used in civil, naval, and aerospace engineering. In topology optimization, the plate and shell elements reduce the analysis time and, consequently, the optimization process [14-17]. In the theory of plates, the plates are classified into thick and thin plates [18]. For thin plates, the shear deformation is neglected, and the Kirchhoff plate theory is used for analysis, but, for thick plates, the shear deformation is considerable, and the Mindlin-Reissner plate theory must be used. The Mindlin-Reissner plate theory for thin plates leads to poor results due to the shear locking phenomenon. To solve the shear locking problem in the Mindlin–Reissner plate theory, (a) the reduced integration method, (b) the natural strain approach, and (c) the stress method have been proposed. A lot of studies have been presented for solving the shear locking problem using these methods, and also new techniques have been introduced. The reduced integration method was used by Zienkiewicz et al. [19] and Pugh et al. [20]. Also, the selective integration method was applied to solve these problems by Malkus and Hughes [21], and also Hughes et al. [22]. Bathe and Dvorkin [23] presented the MITC family. Batoz and Lardeur [20] and also Batoz and Katili [24] developed the Discrete Shear Triangle (DST) family. Choo et al. [25] proposed the hybrid-Trefftz plate elements. The assumed stress/strain elements were used by Lee and Pian [26], Katili [27], and also Brasile [28]. Most of these methods solved the shear locking problem in the plate elements, but these formulations were complex and difficult.

A new three-node triangular plate element, labeled as DST-S6 (Discrete Shear Triangular element with six extra Shear degrees of freedom), was proposed by Cai et al. [29] to analyze the plate/shell structures. The shear locking is eliminated in the DST-S6. In this method, any numerical expediencies (such as the reduced integration, the assumed strains/stresses) are ignored, and a simple formulation was presented. In the same way, Zhuang et al. [30] introduced a new locking-free element triangular thick plate element. In this formulation, each element has nine standard kinematic degrees of freedom and six additional degrees of freedom for shear strains (TTK9S6). This formulation can be used in the analysis of plate and shell structures. They evaluated the performance of TTK9S6 by comparing the obtained central displacement using the FEM with the exact values. As mentioned above, various methods and formulations have been proposed for plate and shell analysis, but the DST-S6 and TTK9S6 formulations presented a simple formulation to calculate the stiffness matrix.

In this paper, a correction function is proposed to modify the bending and shear stiffness matrices of the plate for each element. For this purpose, the TTK9S6 element is used for the plate analysis. In the next section, the TTK9S6 formulation for finite element analysis is presented in detail. In the third section, the correction coefficients of the bending and shear stiffness matrices are introduced. Then, the sensitivity of the central displacement to the bending and shear stiffness matrices is studied. In the fourth section, a correction function is proposed according to the changes of correction coefficients of the bending and shear stiffness matrices. Finally, the performance of the proposed correction function is evaluated throughout several numerical examples. For this purpose, the errors of central displacement for the TTK9S6 and the modified plate element are calculated and compared.

1.1 TTK9S6 Formulation

In this section, the formulation of shape functions, interpolation function, and computing the stiffness matric in terms of bending and shear deformation for the TTK9S6 [30] element is expressed. According to Fig. 1, the total rotations of plates around the x- and y-axis (θ_x and θ_y) without separating the influence of transverse shear deformation are expressed by:

$$\theta_x = \frac{\partial w}{\partial x}, \theta_y = \frac{\partial w}{\partial y} \tag{1}$$

Where w is the vertical displacement. The total rotation includes the rigid body rotation ($\hat{\theta}$) and transverse shear strain (γ). Therefore, the transverse shear strain can be computed as follow:

$$\gamma_x = \theta_x - \hat{\theta}_x, \gamma_y = \theta_y - \hat{\theta}_y \tag{2}$$

The shape functions of TTK9S6 are presented as follows. This element has three main nodes and three additional mid-side nodes, as shown in Fig. 2.

$$\phi_i = L_i,\ \phi_{xi} = \frac{1}{2}(x - x_i)L_i,\ \phi_{yi} = \frac{1}{2}(y - y_i)L_i,\ i = 1,2,3 \tag{3}$$

$$R_i = \left(\sum_{k=4}^{6} N_k\right)\phi_{i,x},\quad R_{xi} = \left(\sum_{k=4}^{6} N_k \phi_{xi,x}^k\right),\quad R_{yi} = \left(\sum_{k=4}^{6} N_k \phi_{yi,x}^k\right),\quad k = 4,5,6 \tag{4}$$

$$Q_i = \left(\sum_{k=4}^{6} N_k\right)\phi_{i,y},\quad Q_{xi} = \left(\sum_{k=4}^{6} N_k \phi_{xi,y}^k\right),\quad Q_{yi} = \left(\sum_{k=4}^{6} N_k \phi_{yi,y}^k\right),\quad k = 4,5,6 \tag{5}$$

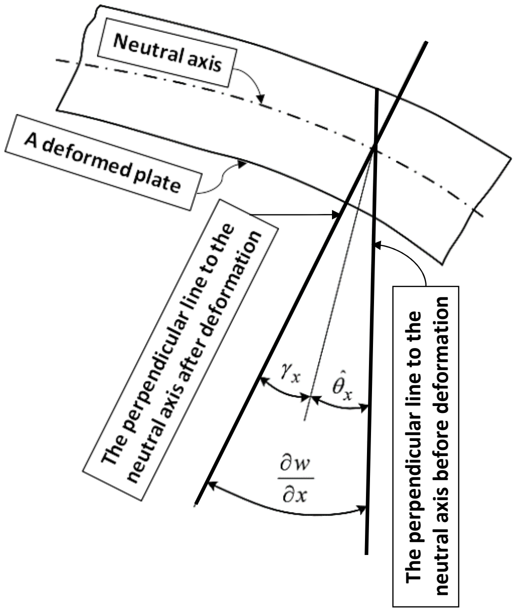

Fig. 1 - Decomposition of total rotation for a plate element

Where i and k are the numbers of main and mid-side nodes, respectively, as shown in Fig. 2. The subscript ",x" denotes the derivatives with respect to x. L_i and N_i are the shape functions of three and six node elements, respectively, that can be calculated by:

$$L_i = \frac{1}{2A}\left(a_i + b_i x + c_i y\right),\ a_i = x_i y_m - x_m y_i,\ b_i = y_j - y_m,\ c_i = x_m - x_j \tag{6}$$

$$2A = \begin{bmatrix} 1 & x_1 & y_1 \\ 1 & x_2 & y_2 \\ 1 & x_3 & y_3 \end{bmatrix} \tag{7}$$

$$N_j = \left(2L_j - 1\right)L_j \ \ \left(j = 1,2,3\right),\ N_4 = 4L_1L_2,\ N_5 = 4L_2L_3,\ N_6 = 4L_3L_1 \tag{8}$$

Also, the derivatives of ϕ_{xi} and ϕ_{yi} with respect to x and y at the mid-side nodes (k=4.5.6) are calculated by:

$$\phi_{xi,x}^{k} = \frac{1}{2}\left[L_i\left(x_k, y_k\right) + \left(x_k - x_i\right)L_{i,x}\right],\ \phi_{yi,x}^{k} = \frac{1}{2}\left[\left(y_k - y_i\right)L_{i,x}\right] \tag{9}$$

$$\phi_{xi,y}^{k} = \frac{1}{2}\left[\left(x_k - x_i\right)L_{i,y}\right],\ \phi_{yi,y}^{k} = \frac{1}{2}\left[L_i\left(x_k, y_k\right) + \left(y_k - y_i\right)L_{i,y}\right] \tag{10}$$

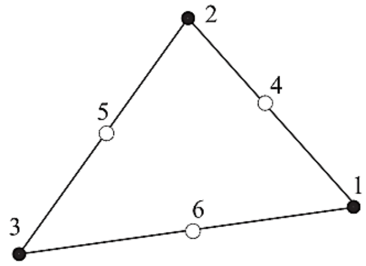

Fig. 2 - TTK9S6 element with three main nodes and three mid-side nodes

The displacements in each element can be calculated approximately as follows:

$$w = \sum_{i=1}^{3} \left(\phi_i w_i + \phi_{xi} \theta_{xi} + \phi_{yi} \theta_{yi} \right) \tag{11}$$

$$\theta_x = \sum_{i=1}^{3} \left(R_i w_i + R_{xi} \theta_{xi} + R_{yi} \theta_{yi} \right) \tag{12}$$

$$\theta_y = \sum_{i=1}^{3} \left(Q_i w_i + Q_{xi} \theta_{xi} + Q_{yi} \theta_{yi} \right) \tag{13}$$

$$\gamma_x = \sum_{i=1}^{3} \left(L_i \gamma_{xi} \right) \tag{14}$$

$$\gamma_y = \sum_{i=1}^{3} \left(L_i \gamma_{yi} \right) \tag{15}$$

The interpolation function of the element can be expressed as follow:

$$U = Nu = \begin{bmatrix} N_1 & N_2 & N_3 \end{bmatrix} \begin{Bmatrix} u_1 \\ u_2 \\ u_3 \end{Bmatrix} \tag{16}$$

Where

$$U = \begin{bmatrix} w & \theta_x & \theta_y & \gamma_x & \gamma_y \end{bmatrix}^T \tag{17}$$

$$u^i = \begin{bmatrix} w_i & \theta_{xi} & \theta_{xi} & \gamma_{xi} & \gamma_{yi} \end{bmatrix}^T \tag{18}$$

$$N_i = \begin{bmatrix} \phi_i & \phi_{xi} & \phi_{yi} & 0 & 0 \\ R_i & R_{xi} & R_{yi} & -L_i & 0 \\ Q_i & Q_{xi} & Q_{yi} & 0 & -L_i \\ 0 & 0 & 0 & L_i & 0 \\ 0 & 0 & 0 & 0 & L_i \end{bmatrix} \tag{19}$$

Now, by determining the interpolation function and using strain energy Π_p for a plate element, the stiffness matrix can be obtained. The strain energy for a plate element is expressed by:

$$\Pi_p = \frac{1}{2} \int_{A_e} \left(\chi^T D_b \chi + \gamma^T D_s \gamma \right) dxdy \tag{20}$$

Where χ and γ are the bending and shear strains vectors, respectively that are defined as follows:

$$\chi = \begin{bmatrix} \dfrac{\partial \theta_x}{\partial x} & \dfrac{\partial \theta_y}{\partial y} & \dfrac{\partial \theta_x}{\partial y} + \dfrac{\partial \theta_y}{\partial x} \end{bmatrix}, \quad \gamma = \begin{bmatrix} \gamma_x & \gamma_y \end{bmatrix} \tag{21}$$

and

$$D_b = \frac{Eh^3}{12\left(1-\upsilon^2\right)} \begin{bmatrix} 1 & \upsilon & 0 \\ \upsilon & 1 & 0 \\ 0 & 0 & \dfrac{1-\upsilon}{2} \end{bmatrix}, \quad D_s = \frac{5Eh}{12\left(1+\upsilon\right)} \begin{bmatrix} 1 & 0 \\ 0 & 1 \end{bmatrix} \tag{22}$$

Where E is Young's modulus, υ is the Poisson's ratio, and h is the thickness of the plate element. Now, the bending and shear stiffness matrices are expressed by:

$$K_b^e = \int_{A_e} B_b^T D_b B_b, \quad K_s^e = \int_{A_e} B_s^T D_s B_s \tag{23}$$

$$B_b = \begin{bmatrix} B_{b1} & B_{b2} & B_{b3} \end{bmatrix} \tag{24}$$

$$B_{bi} = \begin{bmatrix} R_{i,x} & R_{xi,x} & R_{yi,x} & -L_{i,x} & 0 \\ Q_{i,y} & Q_{xi,y} & Q_{yi,y} & 0 & -L_{i,y} \\ R_{i,y}+Q_{i,x} & R_{xi,y}+Q_{xi,x} & R_{yi,y}+Q_{yi,x} & -L_{i,y} & -L_{i,x} \end{bmatrix} \tag{25}$$

$$B_s = \begin{bmatrix} B_{s1} & B_{s2} & B_{s3} \end{bmatrix} \tag{26}$$

$$B_{si} = \begin{bmatrix} 0 & 0 & 0 & L_i & 0 \\ 0 & 0 & 0 & 0 & L_i \end{bmatrix} \tag{27}$$

Finally, the stiffness matrix of the plate element is obtained by adding the bending and shears stiffness matrices as follow:

$$K^e = K_b^e + K_s^e \tag{28}$$

The stiffness matrix can be calculated using Gaussian integration for the bending and shear stiffness matrices as follows:

$$K_b^e = \frac{1}{2}\sum_{m=1}^{n}\left[B_{b(r_m,s_m)}^T D_b B_{b(r_m,s_m)} \omega_m J_{(r_m,s_m)} \right] \tag{29}$$

$$K_s^e = \frac{1}{2}\sum_{m=1}^{n}\left[B_{s(r_m,s_m)}^T D_s B_{s(r_m,s_m)} \omega_m J_{(r_m,s_m)} \right] \tag{30}$$

Where n is the number of Gaussian points, r_m and s_m are the Gaussian points, ω_m is the weight of Gaussian points and $J_{(r_m,s_m)}$ is the Jacobian matrix at the Gaussian points that is calculated by:

$$J = \begin{bmatrix} \frac{\partial X}{\partial x} & \frac{\partial X}{\partial y} \\ \frac{\partial Y}{\partial x} & \frac{\partial Y}{\partial y} \end{bmatrix} \tag{31}$$

Where

$$X = \sum_{i=1}^{6} N_i x_i, \quad Y = \sum_{i=1}^{6} N_i y_i \tag{32}$$

1.2 Investigation of the sensitivity of bending and shear stiffness matrices

In this section, the sensitivity and effects of the bending and shear stiffness matrices on the central deflection of plates are investigated. For this purpose, two coefficients for the bending (α) and the shear (β) stiffness matrices are defined. Thus the K_b^e and K_s^e are expressed as follows:

$$K_b^e = \alpha\frac{1}{2}\sum_{m=1}^{n}\left[B_{b(r_m,s_m)}^T D_b B_{b(r_m,s_m)} \omega_m J_{(r_m,s_m)} \right] \tag{33}$$

$$K_s^e = \beta\frac{1}{2}\sum_{m=1}^{n}\left[B_{s(r_m,s_m)}^T D_s B_{s(r_m,s_m)} \omega_m J_{(r_m,s_m)} \right] \tag{34}$$

Here, the variations of the central deflection of the plate by changing the values of the coefficients are studied to determine the appropriate values for the coefficients (α and β). For investigating the effects of α and β and subsequently K_b^e and K_s^e on the results, a square plate subjected to uniformly distributed surface load (q) is studied. The side length is l, and the thickness of the plate is h. Due to the symmetry of geometry and boundary conditions, only a quarter of the plate is modeled [29, 30], as shown in Fig. 3.

The plate is modeled for a 4×4 and 16×16 mesh size and with clamped and simply supported edges as the boundary conditions. The modulus of elasticity is E=100 (Pa), the side length is equal to l=100 (m), the poison's ratio is υ=0.3, and the uniformly distributed surface load is q=1 (N/m). The thicknesses of plates are equal to h=0.001 (m), 0.1 (m), 1 (m), 10(m), 15(m), and 20(m). The variations of the central deflection with respect to the variations of α (when the β parameter is considered to be constant, β =1) for the plate with 16×16 mesh with clamped and simply supported edges are shown in Fig. 4. It is shown that for h/l=0.2 and 0.15 with the clamped support (Fig. 4 (a)) the values of α must be less than 1 (α<1) but, for the thin plates (h/l =0.1, 0.01, 1e-3, 1e-5), the values of α must be more than 1 (α>1). In the simply supported plate (Fig. 4 (b)), for all values of h/l, α must be more than 1. Fig. 4 (b) shows that the values of α, also increase with an increase in the values of h/l. These results are provided in Fig. 5 for the plate with 4×4 mesh for both clamped and simply supported edges. For the clamped and simply supported plates, the values of α must be more than 1 for convergence to the exact central deflection.

As shown in Fig. 5 (b), increasing the values of h/l leads to an increase in the values of α, but it is inversely for the clamped plate (Fig. 5 (a)). In Fig. 4 and Fig. 5, it is shown that for the thin plates (h/l=0.01,1e-3,1e-5), the values of α will not be changed approximately.

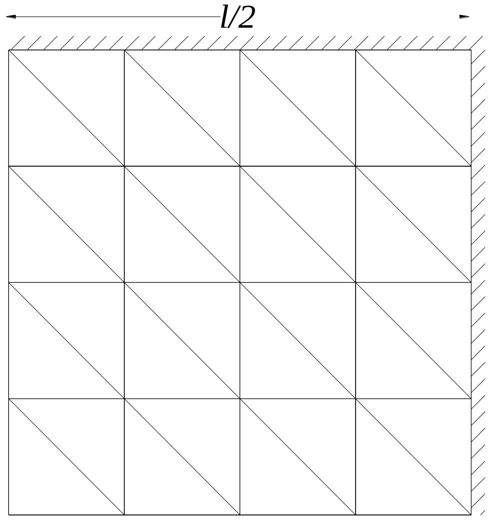

Fig. 3 - Model of a square plate with 8×8 mesh

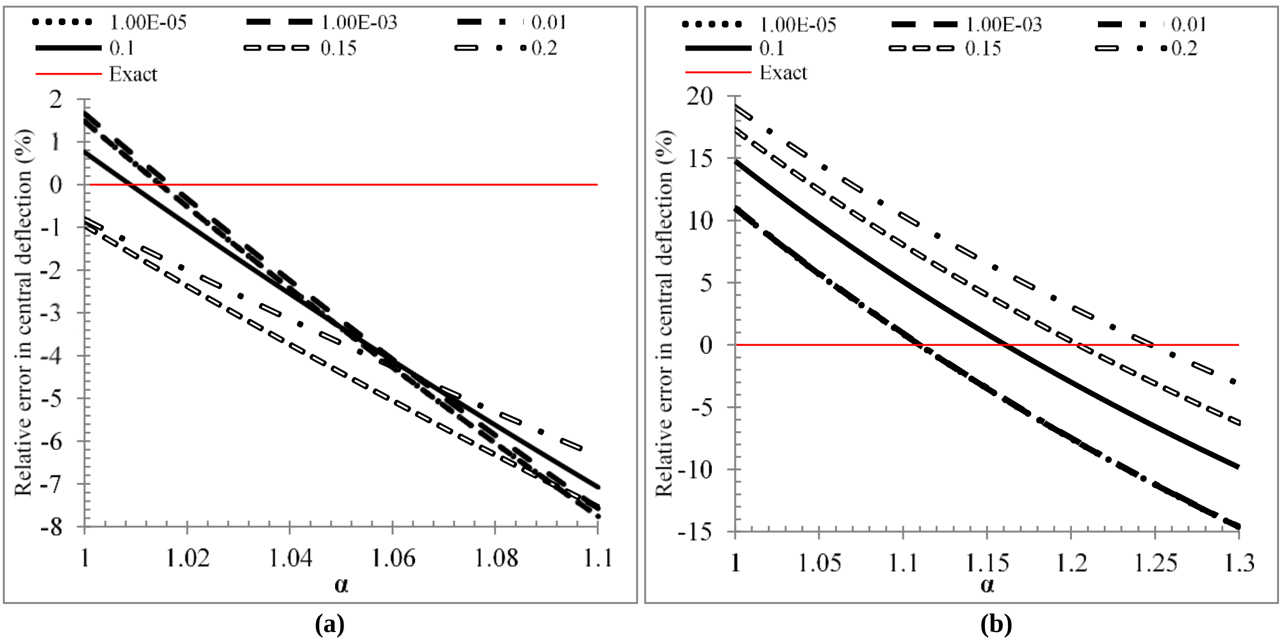

Fig. 4 - Effect of α variations (β=1) on the central deflection for plate with 16×16 mesh, (a) clamped, (b) simply supported

In the following, the variations of the central deflections with respect to variations of the β parameter (when the α parameter is assumed to be constant, α =1) are evaluated. The results for 16×16 and 4×4 mesh are shown in Fig. 6 and Fig. 7, respectively. In Fig. 6 and Fig. 7, it is shown that for thin plates (h/l=0.01,1e-3,1e-5), the variations of β are ineffective on the central deflection values.

As shown in Fig. 6 (a), for 16×16 mesh plate with clamped support edges and h/l=0.2,0.15,0.1, the values of β approximately should be equal to 1 for convergence to the exact values. As shown in Fig. 6 (b), the values of the β should be more than 2 (β>2) for the convergence of the results to the exact values for the thick plates (h/l=0.2, 0.15, 0.1).

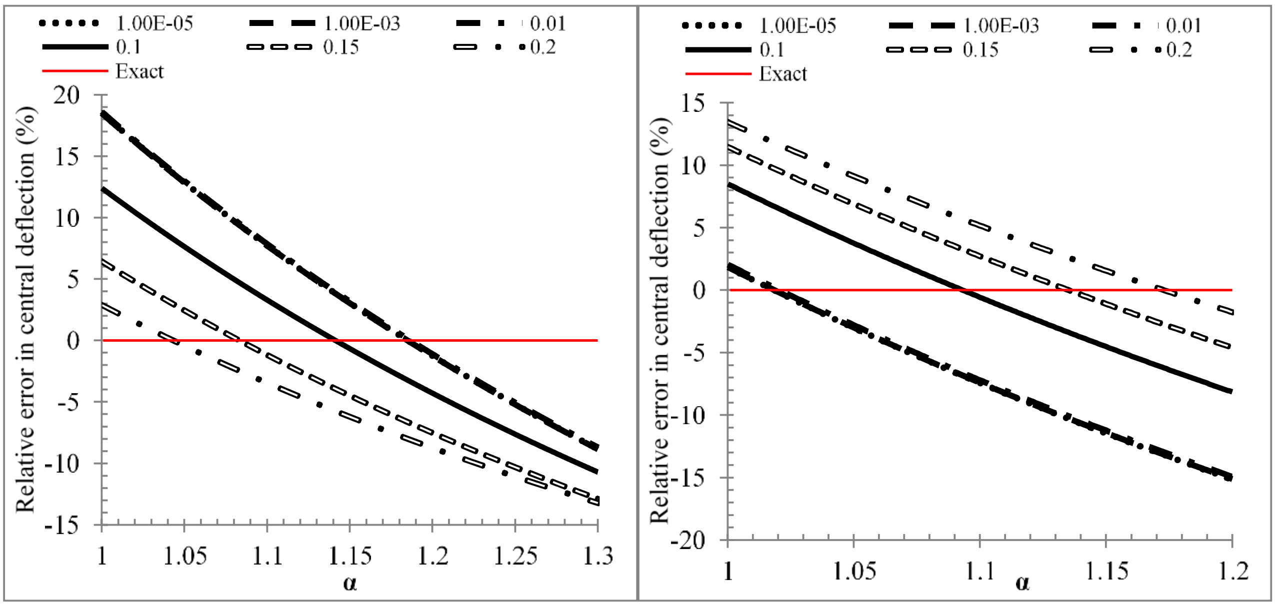

(a) (b)

Fig. 5 - Effect of α variations (*β*=1) on the central deflection for plate with 4×4 mesh, (a) clamped support, (b) simply supported

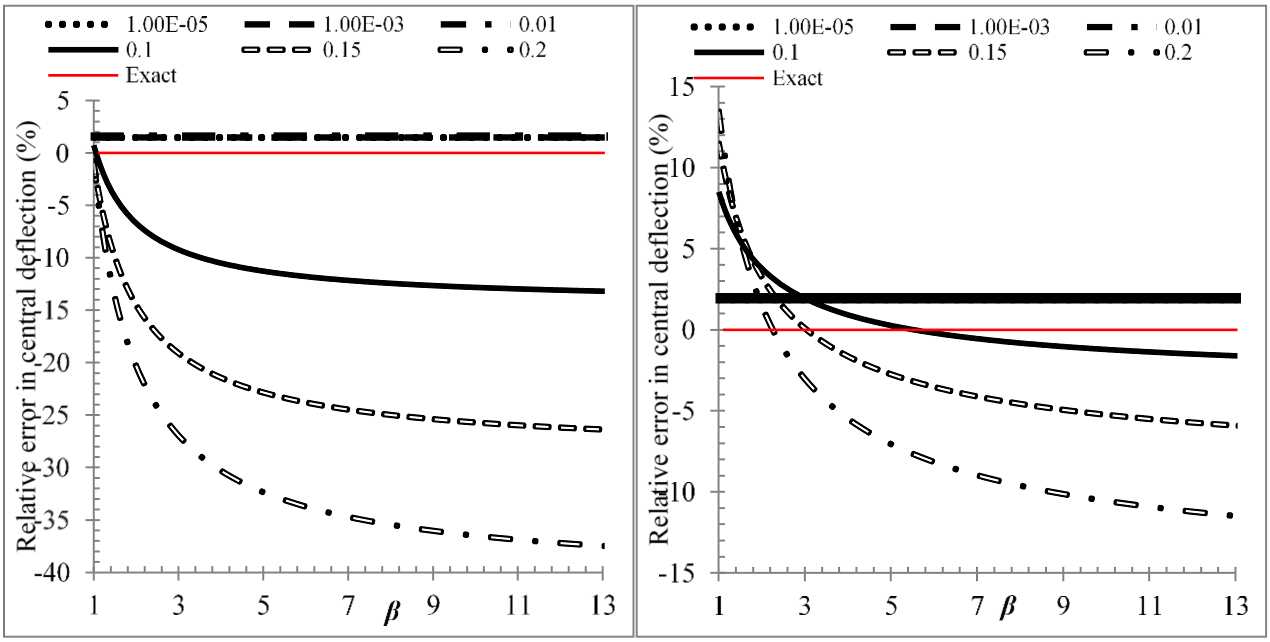

(a) (b)

Fig.6 - Effect of β variations (α =1) on the central deflection of plate with 16×16 mesh, (a) clamped support, (b) simply supported

Fig. 7 (a) shows that only for h/l=0.15 and 0.2, the values of β impact on the values of central deflection. Also, as shown in Fig. 7 (b), only for h/l=0.2, the values of the β parameter can be useful. By comparing Fig. 6 and Fig. 7, it is proved that the β parameter is effective only for the thick plates (h/l=0.2, 0.15, 0.1) and has no effect on the thin plates (h/l=0.01,1e-3,1e-5). Besides, the values of the β parameter are more effective when the mesh size is small, and the plate has simply-supported edges.

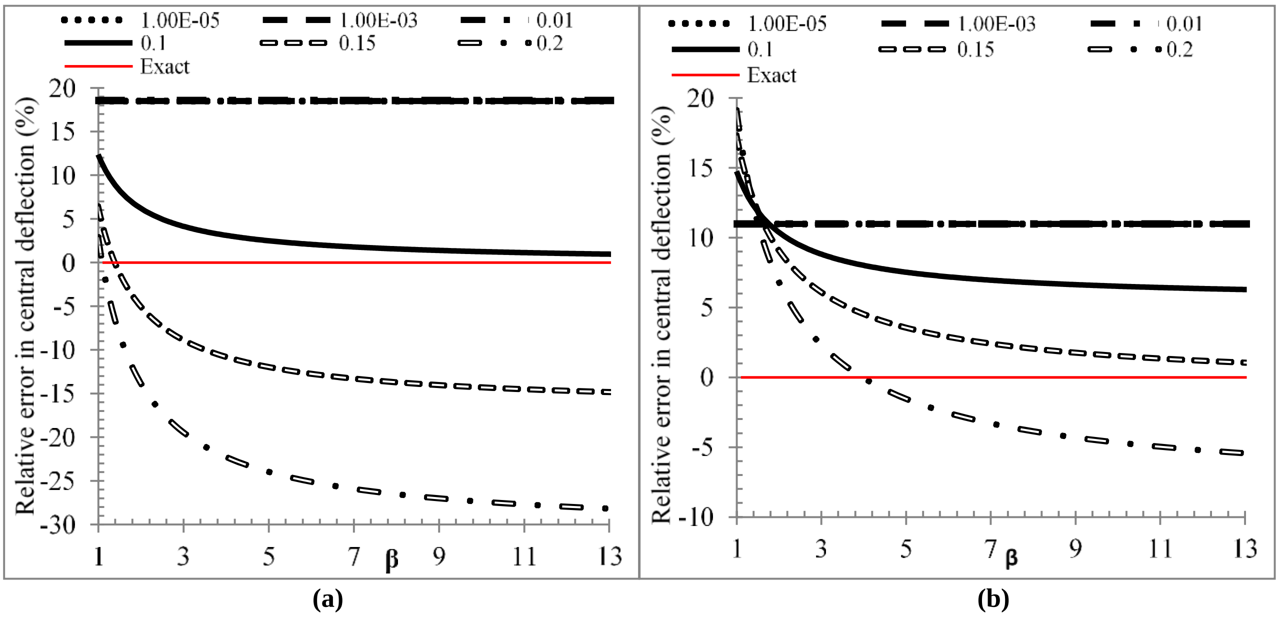

Fig. 7 - Effect of β variations (α =1) on the central deflection of plate with 4×4 mesh, (a) clamped support, (b) simply supported

The sensitivity analysis illustrates that the central displacement of the plate is affected by the flexural stiffness matrix rather than the shear stiffness matrix. The variations of the α parameter indicate that by selecting appropriate values of α and β parameters, the central deflection of the plate can be modified. Consequently, this leads to having a reduction in error values. Choosing a suitable function is complex since the thickness, mesh size, and type of supports can have effects on the results. However, in this paper, using the trial and error method and considering the different scenarios of thickness, mesh size and type of support, a function for α and β parameter is presented as follow:

$$\alpha = \left(\frac{A_t + A_e}{A_t - A_e} \times \frac{A_t - \log\left(h/\sqrt{A_t}\right)}{A_t + \log\left(h/\sqrt{A_t}\right)} \right)^2 , \quad \beta = 1 \tag{35}$$

where A_t is the area of the plate, and A_e is the area of the elements. The bending correction coefficient should be calculated for each element if the area of the elements is not equal. So, the bending matrix is written according to equation (36).

$$K_b^e = \frac{1}{2}\sum_{m=1}^{n}\left[\alpha_m B^T_{b(r_m,s_m)} D_b B_{b(r_m,s_m)} \omega_m J_{(r_m,s_m)}\right] \tag{36}$$

3. Numerical studies

Herein, several numerical studies are presented for evaluating the performance of the proposed modifying function. In the following, the results of TTK9S6 and modified stiffness matrices are presented and compared.

3.1 The circular plate under uniform load

A circular plate under uniform load (q) with clamped or simply supported edges is analyzed to investigate the proposed modifying function. Due to symmetry in the geometry and boundary conditions, only a quarter of the plate is analyzed [29, 30] (Fig. 8).

The modulus of elasticity (E), the radius of the plate (r), and the Poisson's ratio (υ) are 100, 100, and 0.3, respectively. The uniformly distributed surface load is q=1. The plate is modeled for a mesh with 9, 25, 81, 289, and 1089 nodes [30]. The thickness variations are h=0.001, 0.01, 1, 10, 15, and 20. Also, a clamped or simply supported edges are assumed for the boundary conditions of the plate [30]. The results for the clamped and simply supported edges for the plates are listed in Tables 1 and 2, respectively. Note that the results of the modifying function are labeled as "M: means that it has been modified". The results indicate the desirable effects of the modifying function in most cases.

For a better comparison, for the 9-node and 1089-node models, the relative errors in the central deflection with respect to h/l for the clamped and simply supported edges are presented in Fig. 9 (a) and Fig. 9 (b), respectively. These figures show the ability of the proposed function to predict the central deflection.

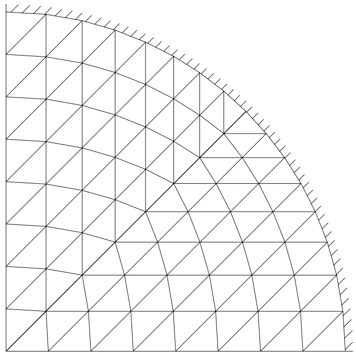

Fig. 8 - 81-node mesh model for a circular plate

Table 1 - Central deflection×(qr4/100D) for circular plate with clamped edges (T:TTK9S6 & M:Modified)

h/*r*	0.00001		0.001		0.01		0.1		0.15		0.2	
models	T	M	T	M	T	M	T	M	T	M	T	M
9n	2.9252	1.7914	2.9252	1.7933	2.9258	1.7948	2.9867	1.8564	3.0635	1.9332	3.1709	2.0405
25n	1.8944	1.6691	1.8944	1.6708	1.8950	1.6723	1.9566	1.7347	2.0343	1.8126	2.1432	1.9216
81n	1.6448	1.5904	1.6448	1.5920	1.6455	1.5935	1.7111	1.6599	1.7940	1.7429	1.9099	1.8590
289n	1.5830	1.5666	1.5830	1.5682	1.5837	1.5697	1.6519	1.6387	1.7380	1.7250	1.8586	1.8457
1089n	1.5676	1.5606	1.5676	1.5622	1.5683	1.5637	1.6378	1.6339	1.7255	1.7218	1.8482	1.8446
Exact	1.5625		1.5625		1.5632		1.6339		1.7232		1.8482	

Table 2 - Central deflection×(qr4/100D) for circular plate with simply edges (T:TTK9S6 & M:Modified)

h/*r*	0.00001		0.001		0.01		0.1		0.15		0.2	
models	T	M	T	M	T	M	T	M	T	M	T	M
9n	8.1234	5.9875	8.1234	5.9936	8.1243	5.9975	8.2160	6.0834	8.3307	6.1865	8.4894	6.3277
25n	6.7936	5.9878	6.7936	5.9939	6.7945	5.9978	6.8775	6.0838	6.9804	6.1869	7.1218	6.3280
81n	6.4757	6.2650	6.4757	6.2714	6.4765	6.2754	6.5548	6.3570	6.6505	6.4531	6.7816	6.5845
289n	6.3966	6.3304	6.3966	6.3369	6.3974	6.3409	6.4723	6.4191	6.5636	6.5109	6.6901	6.6378
1089n	6.3768	6.3482	6.3768	6.3547	6.3776	6.3587	6.4500	6.4343	6.5396	6.5246	6.6649	6.6502
Exact	6.3702		6.3702		6.3709		6.4416		6.5309		6.6559	

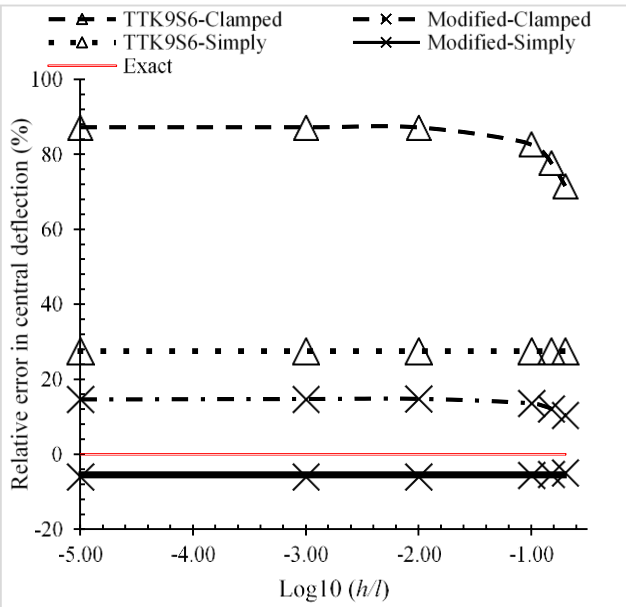

(a)

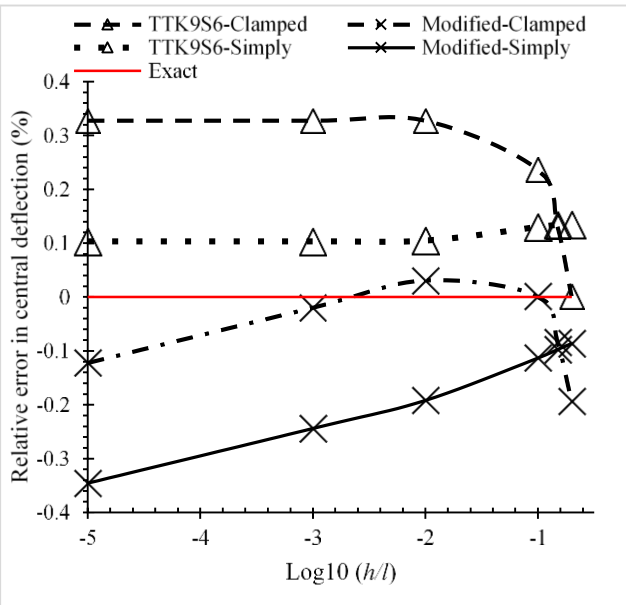

(b)

Fig. 9 - Relative error in central deflection with respect to h/l for the plates with (a) 9-node and (b) 1089-node

3.2 The clamped circular plate under uniform load with different meshes

For further evaluation, two-clamped plates with different meshes are studied here. In the first case, as shown in Fig. 10 (a), the plate has regular mesh with the number of nodes equal to 49. As shown, the area of created elements is different. In the second case, as shown in Fig. 10 (b), the plate has an irregular mesh with the number of nodes equal to 40. The results of the analysis are listed in Table 3. It is shown that the modifying function has an excellent effect on the convergence of the results to the exact values. The relative errors in the central deflection concerning *h*/*l* for 49-node and 40-node meshes are effectively reduced (see Fig. 11).

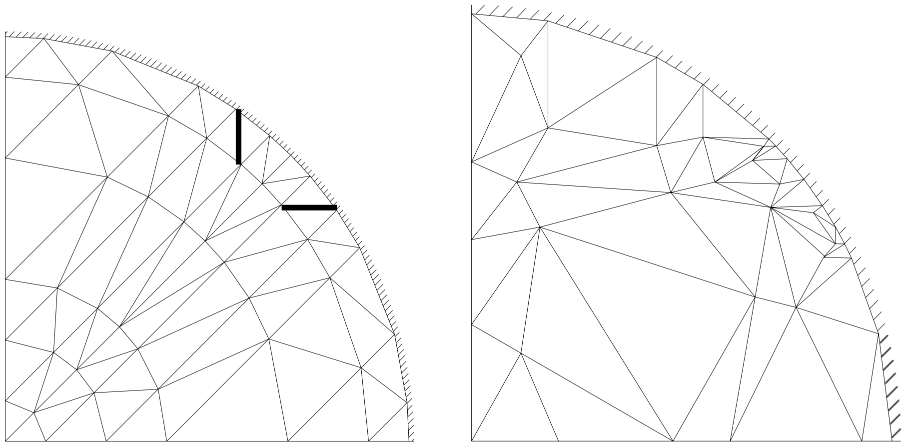

(a) (b)

Fig. 10 - Clamped plate with different meshes (a) 49-node (b) 40-node

Table 3 - Central deflection×(qr4/100D) for a clamped circular plate with different meshes (T: TTK9S6 & M: Modified)

h/*l*	0.00001		0.001		0.01		0.1		0.15		0.2	
models	T	M	T	M	T	M	T	M	T	M	T	M
49n	1.7075	1.6046	1.7075	1.6062	1.7081	1.6077	1.7754	1.6756	1.8600	1.7602	1.9783	1.8783
40n	1.8143	1.5454	1.8143	1.5470	1.8151	1.5486	1.8864	1.6198	1.9726	1.7053	2.0910	1.8225
Exact	1.5625		1.5625		1.5632		1.6339		1.7232		1.8482	

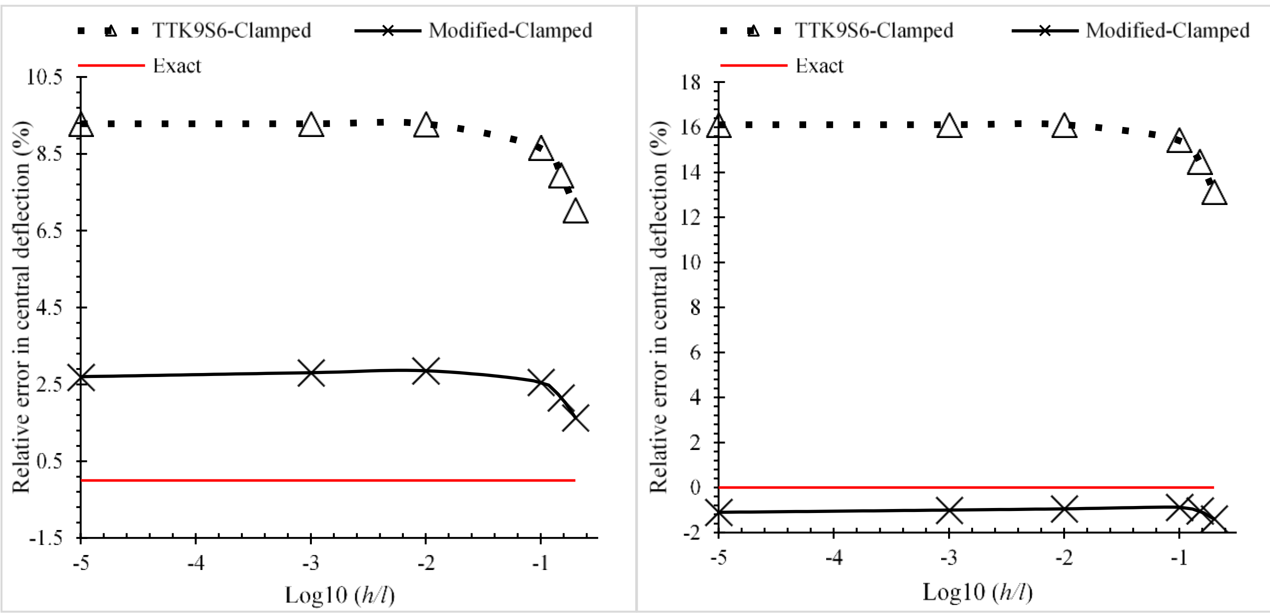

(a) (b)

Fig. 11 - Relative error for evaluation of central deflection with respect to different values for h/l in (a) 49-node and (b) 40-node plates

3.3 The square plate under uniform load

A square plate under uniform load (q) with the clamped or simply supported edges is analyzed for evaluating the proposed modifying function. Due to symmetry in the geometry and boundary conditions, only a quarter of the plate is analyzed (see Fig. 2). The modulus of elasticity is E=100, the length of the plate is l=100, the Poisson's ratio is υ=0.3, and the uniformly distributed surface load is q=1. The plate is modeled with 4×4, 8×8, 16×16, and 32×32 meshes [30]. The thickness variations are assumed to be equal to h=0.001, 0.01, 1, 10, 15, and 20 [30]. The clamped and simply supported edges are considered for the plate. The results of the plates with clamped and simply supported edges are listed in Tables 4 and 5, respectively. Also, the relative errors in computing the central deflection are presented in Fig. 12. As shown in Fig. 12, the effect of modifying function on the errors is reduced when the mesh size is small (16×16).

Table 4 - Central deflection×(ql4/100D) for square plate with clamped edges (T:TTK9S6 & M:Modified)

h/l	0.00001		0.001		0.01		0.1		0.15		0.2	
models	T	M	T	M	T	M	T	M	T	M	T	M
4x4	0.1499	0.1450	0.1499	0.1451	0.1501	0.1454	0.1685	0.1638	0.1914	0.1867	0.2230	0.2183
8x8	0.1334	0.1321	0.1334	0.1322	0.1336	0.1324	0.1546	0.1535	0.1802	0.1791	0.2153	0.2142
16x16	0.1284	0.1279	0.1284	0.1279	0.1286	0.1282	0.1510	0.1507	0.1781	0.1778	0.2149	0.2146
32x32	0.1270	0.1267	0.1270	0.1267	0.1272	0.1271	0.1503	0.1502	0.1780	0.1779	0.2157	0.2156
Exact	0.1265		0.1265		0.1265		0.1499		0.1798		0.2167	

Table 5 - The central deflection×(ql4/100D) for square plate with simply supported (T:TTK9S6 & M:Modified)

h/l	0.00001		0.001		0.01		0.1		0.15		0.2	
models	T	M	T	M	T	M	T	M	T	M	T	M
4x4	0.4508	0.4360	0.4508	0.4364	0.4512	0.4370	0.4904	0.4762	0.5321	0.5177	0.5843	0.5697
8x8	0.4240	0.4121	0.4240	0.4124	0.4246	0.4136	0.4694	0.4626	0.5113	0.5046	0.5626	0.5556
16x16	0.4137	0.4121	0.4137	0.4124	0.4147	0.4136	0.4636	0.4626	0.5056	0.5046	0.5566	0.5556
32x32	0.4096	0.4086	0.4096	0.4089	0.4112	0.4107	0.4622	0.4618	0.5042	0.5038	0.5550	0.5547
Exact	0.4062		0.4062		0.4064		0.4273		0.4536		0.4906	

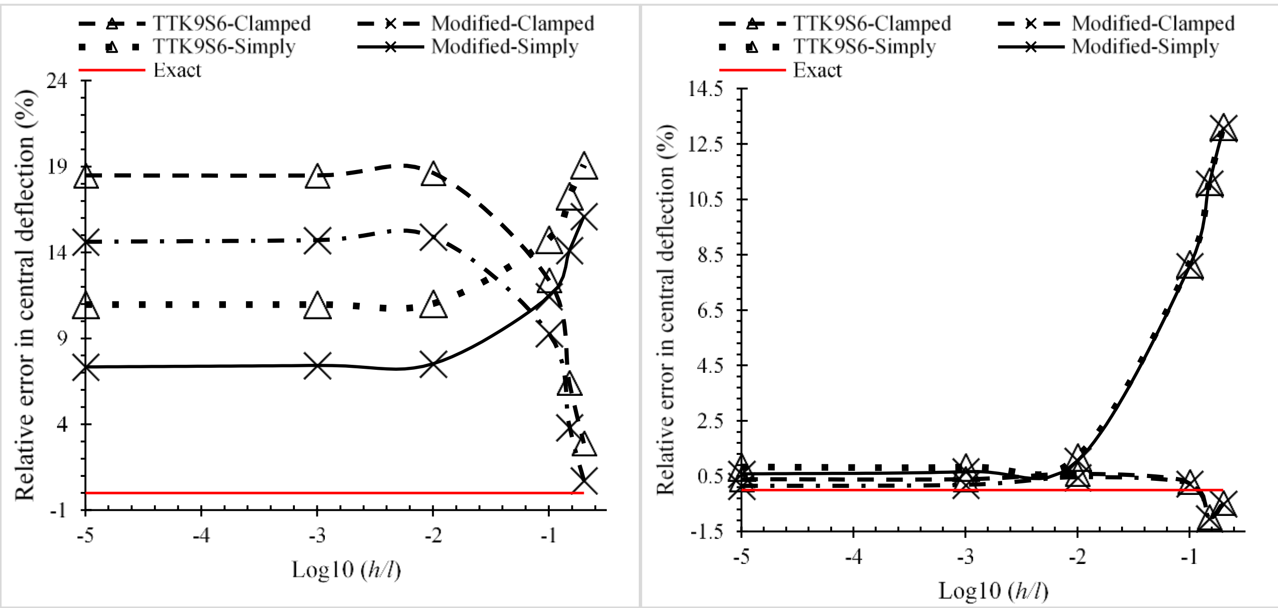

(b) **(b)**

Fig. 12 - Relative error in central deflection with respect to h/l for (a) 4x4 mesh (b) 32x32 meshes

4. Comparing Errors

There are several methods to evaluate the errors, such as mean absolute percentage error (MAPE), root mean square error (RMSE), and so on [31]. For a comprehensive comparison between the results of the TTK9S6 and the modified element, the error percentage (EP) of each element for computing the central displacement in comparison with the exact value is presented in Table 6. The error percentage is calculated in absolute maximum, absolute minimum, and average (MAPE) for each model. It can be seen that the EP in the modified element is significantly decreased. The values of MAPE in the TTK9S6 element (21.57% and 47.32%) are near 5 and 2.8 times the modified element (4.25% and 2.63%) for the circular plates with the clamped and simply supported edges, respectively. The ratios of the MAPE for the square plates with clamped and simply supported edges in the TTK9S6 (4.50% and 8.71%) in comparison with the modified element (3.51% and 7.23%) are equal to 1.28 and 1.20, respectively. So, it is concluded that the effect of the modified element for the reduction of the errors is more considerable in the circular plate. Also, for the clamped circular plate with different meshes, the significant effect can be seen in the error reduction for the modified element (Table 3). As shown, the values of MAPE for the TTK9S6 and modified elements are equal to 11.91 and 1.75, respectively. It means that the MAPE in TTL9S6 is approximately 6.81 times the modified element. The results also illustrate a significant reduction in the maximum EP. As shown in Table 6, the maximum EP for the TTK9S6 is equal to 87.21%, while this value is 16.13% for the modified element.

Table 6 - Error percentage (%) of TTK9S6 and modified element

Models	Maximum		Minimum		Average (MAPE)	
	TTK9S6	Modified	TTK9S6	Modified	TTK9S6	Modified
Clamped circular plate (Table 1)	87.21	14.81	0.00	0.00	21.57	4.25
Simply supported circular plate (Table 2)	27.56	6.01	0.10	0.09	7.32	2.63
Clamped circular plate with different meshes (Table 3)	16.12	2.85	7.04	0.86	11.91	1.75
Clamped square plate (Table 4)	18.64	14.91	0.23	0.15	4.50	3.51
Simply supported square plate (Table 5)	19.10	16.13	0.83	0.58	8.71	7.23
All models	87.21	16.13	0.00	0.00	11.06	4.04

5. Conclusion

In this paper, an idea was suggested to improve the results of plate elements based on the coefficient correction. The results of the sensitivity analysis proved that the central displacement depends on the bending stiffness matrix, and the effects of shear stiffness matrix could be ignored. According to the variations of the correction factor for the bending stiffness, a function was proposed. The results indicated that in most cases, the proposed modifying function caused to converge the central displacements to the exact values, and the errors were reduced. The investigations showed that in the plates with large mesh and also with irregular mesh, the proposed function effectively reduced the errors. The results of different numerical examples illustrated that the use of the bending correction factor averagely decreases the errors of FEM analysis from 11.06% to 4.04%

Acknowledgement

The authors would like to acknowledge the Shahid Rajaee Teacher Training University and Shahrekord University.

References

[1] Clovgh, R.W., & Tocher, J.L. (1966). Finite element stiffness matrices for analysis of plates in bendingProceedings of Conference on Matrix Methods in Structural Mechanics, Ohio, USA. 515-541.

[2] Choi, C.-K., & Kwak, H.-G. (1990). The effect of finite element mesh size in nonlinear analysis of reinforced concrete structures. Computers & Structures, 36(5), 807-815.

[3] Kanapady, R., Bathina, S., Tamma, K., Kamath, C., & Kumar, V. (2001). Determination of an initial mesh density for finite element computations via data mining. CA (US): Lawrence Livermore National Lab

[4] Li, Y., Karr, D.G., & Wang, G. (2007). Mesh size effects in simulating ductile fracture of metalsProceedings of 10th International Symposium on Practical Design on Ships and Other Floating Structures. Houston, Texas United States of America, 247-254.

[5] Nam, J.W., Kim, J.-H.J., Kim, S.B., Yi, N.H., & Byun, K.J. (2008). A study on mesh size dependency of finite element blast structural analysis induced by non-uniform pressure distribution from high explosive blast wave. KSCE Journal of Civil Engineering, 12(4), 259-265.

[6] Troyani, N., Perez, A., & Baiz, P. (2005). Effect of finite element mesh orientation on solution accuracy for torsional problems. Finite elements in analysis and design, 41(14), 1377-1383.

[7] Suresh, K., & Regalla, S.P. (2014). Effect of mesh parameters in finite element simulation of single point incremental sheet forming process. Procedia materials science, 6, 376-382.

[8] Antunes, F., Camas, D., Correia, L., & Branco, R. (2015). Finite element meshes for optimal modelling of plasticity induced crack closure. Engineering Fracture Mechanics, 142, 184-200.

[9] Perumal, L. (2019). New approaches for Delaunay triangulation and optimisation. Heliyon, 5(8), e02319.

[10] Kamgar, R., Gholami, F., Zarif Sanayei, H.R., & Heidarzadeh, H. (2019). Modified tuned liquid dampers for seismic protection of buildings considering soil-structure interaction effects. Iranian Journal of Science and Technology, Transactions of Civil Engineering, 1-16.

[11] Tavakoli, R., Kamgar, R., & Rahgozar, R. (2019). Seismic performance of outrigger-braced system based on finite element and component-mode synthesis methods. Iranian Journal of Science and Technology, Transactions of Civil Engineering, 1-9.

[12] Majlan, E.H., Daud, W.R.W., Husaini, T., Rosli, M.I., Sulong, A.B., & Sebayang, D. (2019). Finite Element Analysis for Stress Distribution in a Proton Exchange Membrane Fuel Cell Stack. International Journal of Integrated Engineering, 11(7), 233-240.

[13] Zakwan, F.A.A., Krishnamoorthy, R.R., Ibrahim, A., & Ismail, R. (2018). A Finite Element (FE) simulation of naked solid steel beam at elevated temperature. International Journal of Integrated Engineering, 10(9), 96-102.

[14] Bagherinejad, M.H., & Haghollahi, A. (2018). Topology optimization of steel plate shear walls in the moment frames. Steel and Composite Structures, 29(6), 771-783.

[15] Bagherinejad, M.H., & Haghollahi, A. (2019). Topology optimization of perforated steel plate shear walls with thick plate in simple frames. International Journal of Optimization in Civil Engineering, 9(3), 457-482.

[16] Gholizadeh, S., & Shahrezaei, A.M. (2015). Optimal placement of steel plate shear walls for steel frames by bat algorithm. The Structural Design of Tall and Special Buildings, 24(1), 1-18.

[17] Haruyama, S., Choiron, M.A., & Nurhadiyanto, D. (2019). Optimum Design of Laminated Corrugated Metal Gasket Using Computer Simulation. International Journal of Integrated Engineering, 11(5), 29-34.

[18] Krishnamoorthy, C. (1994). Finite element analysis: theory and programming. Tata McGraw-Hill Education.

[19] Zienkiewicz, O., Taylor, R., & Too, J. (1971). Reduced integration technique in general analysis of plates and shells. International Journal for Numerical Methods in Engineering, 3(2), 275-290.

[20] Pugh, E., Hinton, E., & Zienkiewicz, O. (1978). A study of quadrilateral plate bending elements with ‘reduced’ integration. International Journal for Numerical Methods in Engineering, 12(7), 1059-1079.

[21] Malkus, D.S., & Hughes, T.J. (1978). Mixed finite element methods-reduced and selective integration techniques: a unification of concepts. Computer Methods in Applied Mechanics and Engineering, 15(1), 63-81.

[22] Hughes, T.J., Cohen, M., & Haroun, M. (1978). Reduced and selective integration techniques in the finite element analysis of plates. Nuclear Engineering and Design, 46(1), 203-222.

[23] Bathe, K.J., & Dvorkin, E.N. (1985). A four-node plate bending element based on Mindlin/Reissner plate theory and a mixed interpolation. International Journal for Numerical Methods in Engineering, 21(2), 367-383.

[24] Batoz, J.L., & Katili, I. (1992). On a simple triangular Reissner/Mindlin plate element based on incompatible modes and discrete constraints. International Journal for Numerical Methods in Engineering, 35(8), 1603-1632.

[25] Choo, Y.S., Choi, N., & Lee, B.C. (2010). A new hybrid-Trefftz triangular and quadrilateral plate elements. Applied Mathematical Modelling, 34(1), 14-23.

[26] Lee, S., & Pian, T. (1978). Improvement of plate and shell finite elements by mixed formulations. AIAA Journal, 16(1), 29-34.

[27] Katili, I. (1993). A new discrete Kirchhoff-Mindlin element based on Mindlin-Reissner plate theory and assumed shear strain fields—part I: An extended DKT element for thick-plate bending analysis. International Journal for Numerical Methods in Engineering, 36(11), 1859-1883.

[28] Brasile, S. (2008). An isostatic assumed stress triangular element for the Reissner-Mindlin plate-bending problem. International Journal for Numerical Methods in Engineering, 74(6), 971-995.

[29] Cai, Y., Tian, L., & Atluri, S. (2011). A simple locking-free discrete shear triangular plate element. Computer Modeling in Engineering & Sciences(CMES), 77(3-4), 221-238.

[30] Zhuang, X., Huang, R., Zhu, H., Askes, H., & Mathisen, K. (2013). A new and simple locking-free triangular thick plate element using independent shear degrees of freedom. Finite Elements in Analysis and Design, 75, 1-7.

[31] Kamgar, R., Bagherinejad, M.H., & Heidarzadeh, H. (2019). A new formulation for prediction of the shear capacity of FRP in strengthened reinforced concrete beams. Soft Computing, 1-17.